Nonperturbative RG treatment of amplitude fluctuations for $|\varphi|^4$ topological phase transitions

Nicolò Defenu,[1] Andrea Trombettoni,[2,3] István Nándori,[4,5,6] and Tilman Enss[1]

[1] *Institut für Theoretische Physik, Universität Heidelberg, D-69120 Heidelberg, Germany*
[2] *CNR-IOM DEMOCRITOS Simulation Center, Via Bonomea 265, I-34136 Trieste, Italy*
[3] *SISSA and INFN, Sezione di Trieste, Via Bonomea 265, I-34136 Trieste, Italy*
[4] *MTA-DE Particle Physics Research Group, P.O.Box 51, H-4001 Debrecen, Hungary*
[5] *MTA Atomki, P.O.Box 51, H-4001 Debrecen, Hungary*
[6] *University of Debrecen, P.O.Box 105, H-4010 Debrecen, Hungary*

(Dated: June 5, 2017)

The study of the Berezinskii-Kosterlitz-Thouless (BKT) transition in two-dimensional $|\varphi|^4$ models can be performed in several representations, and the amplitude-phase (AP) Madelung parametrization is a natural way to study the contribution of density fluctuations to non-universal quantities. We show how one can obtain a consistent phase diagram in the AP representation using the functional renormalization group scheme. Constructing the mapping between $|\varphi|^4$ and the XY models allows us to treat these models on equal footing. We estimate universal and non-universal quantities of the two models and find good agreement with available Monte Carlo results. The presented approach is flexible enough to treat parameter ranges of experimental relevance.

arXiv:1706.00618v1 [cond-mat.quant-gas] 2 Jun 2017

I. INTRODUCTION

The study of topological phase transitions plays a major role in modern physics, both for the importance of having non-local order parameters in absence of conventional spontaneous symmetry breaking and for their occurrence in a wide variety of low-dimensional systems, including superfluid[1] and superconducting films[2], two-dimensional ($2d$) superconducting arrays[3–5], granular superconductors[6], $2d$ cold atomic systems[7–9] and one-dimensional ($1d$) quantum models[10].

The nowadays standard understanding of the main properties of phase transitions in $2d$ interacting systems is based on the role of topological defects[11], encoding the relevant excitations of these models. In $2d$ systems with continuous symmetry the unbinding of vortex excitations drives the system out of the superfluid state above a finite critical temperature $T_{\rm BKT}$. The mechanism for this topological phase transition in $2d$ with continuous symmetry—in which there is no local order parameter according to the Mermin-Wagner (MW) theorem[12,13]—was first explained by Berezinksii, Kosterlitz and Thouless[14–16] and lead to the paradigm of the BKT critical behavior, which was recognized with the 2016 Nobel prize[17,18].

The importance of the BKT mechanism can hardly be overestimated. On the one hand, it explained $2d$ superfluidity at finite temperature despite the lack of off-diagonal long-range order[19], which manifests itself in the absence of magnetization in $2d$ magnetic models such as the XY model[12] and in a vanishing condensate fraction at finite temperature in $2d$ bosonic models[20]. Nevertheless, because of the power-law decay of correlation functions in the low-temperature phase[14] one can still have superfluid/superconducting behavior[21]. The physical consequences have been studied in very different $2d$ systems, with applications ranging from soft matter[11] and magnetic systems[22] to layered and high-T_c superconductors[23], where the strong anisotropy[24] may induce BKT behavior[23,25]; for an overview of the relevant literature we refer the reader to the recent review[17]. At the same time, despite extensive work the effects of disorder, spatial anisotropy and more complex or long-range interactions in real systems require the development of advanced theoretical tools to extend our knowledge and treatment of BKT topological phase transitions to these cases.

On the other hand, $1d$ quantum systems at zero temperature can be mapped via the quantum-to-classical correspondence to $2d$ classical models at finite temperature and share the same universal properties. This motivated extensive study of BKT properties in $1+1$ dimensional models and field theories, in particular the sine-Gordon (SG) model[26,27]. The XY model can be linked to SG theory in two steps: first, the Villain approximation[28] to the XY model preserves the periodicity of the phase variable but approximates the cosine angular dependence with a harmonic one, and can be mapped exactly onto the $2d$ Coulomb gas[29–31]. It was shown rigorously[32] that both the Coulomb gas and the Villain model exhibit a BKT transition. In a second step, the Coulomb gas is mapped onto the SG model by neglecting irrelevant higher vorticities/charges, and exhibits a BKT transition at the critical point $\beta^2 = 8\pi$[26,33,34]. In the Villain model, vortex and spin-wave degrees of freedom are decoupled, unlike in the XY model[35]. We stress that in general a strong spin-vortex coupling may destroy the BKT transition.

An important comment is that the BKT scenario works when one can define local phases and explicitly detect and study vortices, such as in the $2d$ XY model on a lattice, but it also applies when it is difficult to define the phase or detect vortices. In all cases, the BKT transition separates a low-temperature phase with power-law decaying correlations from a high-temperature phase with exponentially decaying correlations, without an explicit need to monitor vortex configurations[7]. However, the fact that one need not explicitly introduce vortices does not mean one can disregard the periodic (compact) nature of the phase variables, which is crucial to obtain the BKT transition. This is correctly taken into account in the SG model, and without periodicity of the phase no BKT transition is found. This subtlety of defining the phase is the reason why the results from the SG and $|\varphi|^4$ models are not easily related: the SG model provides an excellent description of the RG flow near the critical point and it is the natural formalism to include the compact nature of the phase, but the inclusion of fluctuations apart from vortices is not straightforward. In contrast, within the $O(2)$ symmetric $|\varphi|^4$ theory one readily estimates η, but it is difficult to access the properties related to the periodicity of the phase and to recover the known expected behaviour in the thermodynamic limit (see below).

In this work we discuss the role of the phase variable in $|\varphi|^4$ theory and show that the amplitude-phase (AP) Madelung representation of the field $\varphi = \sqrt{\rho}\, e^{i\theta}$ leads to a consistent and efficient treatment combining the advantages of the SG and $|\varphi|^4$ approaches. With this tool we can treat on equal footing both the XY lattice model, where amplitude is fixed by construction, and the $|\varphi|^4$ model, for which we demonstrate without *a priori* assumptions that amplitude (density) fluctuations are gapped at the critical point. For this purpose we employ an exact mapping from the XY model to an appropriate $|\varphi|^4$ theory. Our approach with a periodic phase variable recovers the universal properties of the BKT transition including essential scaling and the equation of state in the fluctuation regime; this would be lost without phase periodicity. More importantly, we can also study the contribution of amplitude and longitudinal spin fluctuations to non-universal quantities such as the critical temperature, which is useful for BKT studies of $2d$ superconductors[36,37] and other materials.

We perform our study in the framework of the functional renormalization group (FRG), which generalizes the idea of Wilson renormalization to the full functional form of the Landau-Ginzburg free energy. Since its introduction[38], FRG has been able to recover and expand most of the traditional RG results and provides a systematic approach for the investigation of high-energy[39], condensed matter[40–42] and statistical physics[43]. An advantage of FRG is particularly evident when considering the universal critical exponents of $O(N)$ field theories as a function of the spatial dimension d and the field component number N. The FRG approach combined with lowest order derivative expansion[44] is able to produce numerical curves for the critical exponent η and ν, respectively the anomalous dimension and the correlation length exponent, which reproduce the expected behavior in the limiting cases $N \to \infty$, $d \to 4$ and $d \to 2$[45,46]; also $O(N)$ models with long-range interaction have been studied[47,48].

Since several works already addressed the BKT transition using FRG[49–55], we think it is useful to explain here in detail our motivation to study $2d$ systems in an FRG framework using our AP parameterization. FRG reproduces for $d \to 2$ the exact behavior provided by the MW theorem[12,13]. Moreover, it is possible to recover the MW theorem already at the lowest order of the derivative expansion, *i.e.*, in the local potential approximation[56]. The compatibility of FRG results with the MW theorem also leads in the $N > 2$ case to an exact agreement of numerical critical exponents with the lowest order $4-\varepsilon$[57] and $2+\tilde{\varepsilon}$ expansion[58] for the $O(N)$ non-linear σ-models. Furthermore, for the anomalous dimension η in general d one gets $\eta \to 0$ for $d > 2$ and $N \geq 2$ in the limit $d \to 2$[45,46]. However, in the BKT case $d = 2$ and $N = 2$, the application of FRG is much less straightforward.

The field theoretical and FRG approaches to the $d = 2$, $N = 2$ case in general use a two-component, complex $|\varphi|^4$ theory in the continuum. The field φ entering the partition function can be parametrized in the following ways:

(i) the field and its complex conjugate, φ and φ^*;

(ii) the real and imaginary parts of φ, *i.e.*, $\mathrm{Re}\,\varphi$ and $\mathrm{Im}\,\varphi$;

(iii) the amplitude ρ and the phase θ of the field $\varphi = \sqrt{\rho}\, e^{i\theta}$.

In the paper[49] the $|\varphi|^4$ model in $d = 2$ is studied within FRG by the derivative expansion formalism using the parametrization (i), where the phase periodicity is implicitly implemented. Proceeding in this way, one can show that there is a line of (pseudo)-fixed points, which is a hallmark of BKT, and η can be estimated in good agreement with the BKT prediction[49], even though it is not possible to unambiguously locate the critical point. Indeed, in order to locate the critical point it is necessary to terminate the FRG flow at a finite momentum, corresponding to a reasonable (but arbitrary) size of the system as also used in[51]. The β-function for the interaction coupling λ obtained in this FRG scheme agrees with the one of the non-linear σ-model only at first order in T. This discrepancy leads to a rather different behavior: in the loop expansion of the non-linear σ model the flow of the interaction λ is trivial, since all loop contributions vanish, and the model remains always in its low-temperature phase. On the other hand, the FRG treatment gives a nontrivial flow for the λ coupling with a line of pseudo-fixed points appearing at low temperature and a high-temperature phase were the system renormalizes to a symmetric state. In[49] this behavior is interpreted as a clue of BKT behavior, since the system presents a low-temperature ordered phase where the interaction coupling remains finite at low energy scales, while the system is driven to a disordered phase $\lambda = 0$ for large temperature values. However, the low-temperature pseudo-fixed point line in the FRG behavior is unstable and the system is always driven to the high temperature state in the thermodynamic limit, in contradiction with the traditional BKT picture. We stress that a similar contradiction also appears in the Migdal treatment of the $2d$ XY model, as pointed out already in the 1970's[29].

Subsequently, the analysis present in[49] has been complemented and extended both with more advanced functional truncations[50,55] and with a detailed regulator analysis[54]. The findings in[50,55] confirm also at higher approximation level the scenario presented in[49]. In[54], using the representation (i), a line of true fixed points is found after performing an optimization of the regulator for each initial condition of the RG flow. By introducing a fine-tuned temperature-dependent regulator, very good results are found for the anomalous dimension and the jump of the stiffness at $T_{\rm BKT}$[54].

Regarding parametrization (ii), we observe that in[55] it is reported that if one disregards the real part of φ then one finds the BKT scenario, due to the implicit assumption of gapped spin-wave excitations. It would be however desirable to have an approach where such assumption is not done, also in view of studying more complex cases in which the existence of the BKT transition is not *a priori* known. Since BKT physics is recovered in the transverse excitation channel, the inclusion of longitudinal modes destroys the exact line of fixed points driving the RG flow to the high temperature phase for all initial conditions[55]. This picture may suggest instability of the low temperature ordered phase due to the interplay of massless transverse modes with the massive longitudinal mode. The valuable investigation of[55] suggests that one needs to discard the instability found in the fixed point line in order to obtain a consistent treatment of the BKT universality class.

The previous discussion shows the remarkable advantages, as well as drawbacks, of using FRG with the (equivalent) parametrizations (i) and (ii) for the study of BKT transitions. The goal of the present paper is to show that the AP parametrization (iii) provides a natural way to overcome possible ambiguities obtained using the other parametrizations and to show that vortices remain bound below the transition for the XY and $|\varphi|^4$ models without any *ad hoc* assumption on the existence and validity of the BKT transition itself. When the phase θ is treated as a non-periodic variable (unlike what it is done in the SG model) then one has only the low-temperature phase and no BKT transition. The key point is to implement the periodicity of the phase: when this is done with density ρ constant, one obtains the SG theory, but one can also consider non-constant ρ, which allows one to compare with available numerical results for the $|\varphi|^4$ model[59–62]. We show in the following that our approach recovers the universality of thermodynamic functions[59,60,62–65]. A further advantage of the use of the AP parametrization is that one can treat the XY and $|\varphi|^4$ models on equal footing and show that amplitude excitations are gapped at criticality. Using the consolidated methods of FRG, one can then find estimates of non-universal quantities of the two models, including a discussion of the effect of longitudinal and amplitude fluctuations on the superfluid/spin stiffness.

II. THE MODELS AND DISCUSSION OF PREVIOUS FRG RESULTS

In this section we introduce the XY and $|\varphi|^4$ models studied in this work and recapitulate basic properties of the BKT phase transition. We then discuss previous FRG work before presenting our results in Sections IV-V.

A. The XY and $|\varphi|^4$ models in $2d$

The Hamiltonian of the XY or plane rotor model reads

$$\beta H_{XY} = -K \sum_{\langle ij \rangle} \left[\cos\left(\theta_i - \theta_j\right) - 1\right] \tag{1}$$

where $K = \beta J > 0$ denotes the spin coupling in units of temperature and as usual $\beta = 1/k_B T$. The angles θ_i are defined at the sites i of a $2d$ lattice; in the following we consider square lattices. The ground state is fully magnetized with all spins pointing in the same direction, $\theta_i = \theta_0 \, \forall \, i$, and is infinitely degenerate. At any $T > 0$ symmetry breaking is forbidden in $2d$ by the MW theorem. Nevertheless, finite systems can have a nonzero magnetization, which is used to detect the BKT transition[66]. In ultracold atomic gases the counterpart of the magnetization is the $\boldsymbol{k} = 0$ component of the momentum distribution and the central peak of the atomic density profile sharply decreases around $T_{\rm BKT}$[67].

The action for the $|\varphi|^4$ model reads

$$S[\varphi] = \int d^2x \left\{ \frac{1}{2} \partial_\mu \varphi \partial_\mu \varphi^* - \mu |\varphi|^2 + \frac{U}{2} |\varphi|^4 \right\} \tag{2}$$

Note that in Eq. (2) we have set the mass $m = 1$, but when useful we will restore it. We shall use units in which $\hbar = k_B = 1$.

Continuous $O(N)$ field theories, with the action (2) corresponding to $N = 2$, have been studied intensively and provide traditional examples of the field theoretical treatment of phase transitions. The nonperturbative FRG has produced a comprehensive picture of the universality classes of such theories for every real dimension d and number of field components N[45,46]. In Section III we discuss how to map the XY model (1) into the $|\varphi|^4$ model (2).

To fix the notation and state results used later, we briefly recapitulate basic results of the BKT universality class[68] referring to the XY model. A discussion of BKT theory in the $|\varphi|^4$ model can be found, e.g., in[60]. Within a spin-wave analysis of the XY model (1), we can expand around the symmetry broken state for small phase displacements $\theta_i - \theta_j \ll 1$, which in the continuum limit leads to

$$\beta H_{\rm sw} = \frac{K}{2} \int \left(\nabla \theta\right)^2 d^2x. \tag{3}$$

When the phase θ is treated as periodic the latter model is equivalent to the Villain model[28]. Neglecting the compactness of phase variable θ, one readily finds

$$M_L \propto \left(\frac{a}{L}\right)^{\frac{1}{2\pi K}}, \quad G(x) \propto \left(\frac{a\pi}{x}\right)^{\frac{1}{2\pi K}}, \tag{4}$$

where M_L is the magnetization of a finite system of size L and lattice spacing a, and $G(x)$ denotes the two-point correlation function between two spins at distance x in the thermodynamic limit (see App. A for a derivation).

The magnetization (4) decays as a power law of the system size, and in the thermodynamic limit the system has no finite order parameter at finite temperature, in agreement with the MW theorem. On the other hand, the two-point correlation (4) displays algebraic behavior with temperature dependent anomalous dimension

$$\eta(T) = \frac{T}{2\pi J}. \tag{5}$$

This result is generally valid also at higher order in the low temperature expansion of the system.

The spin-wave analysis suggests that the ordered phase is stable at all temperatures and the correlation functions have power-law behavior even for small K values. However, this is inconsistent with an intuitive argument[15] based on the free energy $F = (\pi J - 2T)\log\left(\frac{L}{a}\right)$ of a macroscopic vortex configuration (see, e.g.,[35]). Accordingly, vortex configurations of the spin should become favorable for temperatures larger than

$$T_{\mathrm{BKT}} \approx \frac{\pi J}{2}. \tag{6}$$

For $T > T_{\mathrm{BKT}}$, one expects vortex excitations to proliferate and destroy the long-range order found in the spin-wave analysis. Monte Carlo simulations have established $T_{\mathrm{BKT}} \simeq 0.893J$[69–73]. A review of the critical properties of the Villain model is provided in[74], and for comparison its critical temperature is $\simeq 1.330J$[75].

The continuous field theory for the spin-wave approximation is, however, not suited to account for vortex configurations, which are characterized by

$$\oint_C \nabla\theta = 2\pi m_i \tag{7}$$

when integrating over a closed contour C. The single-valued complex field φ allows for differences in the phase field θ by multiples of 2π, and thereby imposes the condition $m_i \in \mathbb{Z}$ for the winding number of the vortex configurations. Instead, the path integral formulation with a single-valued field θ does not include vortex configurations.

It is possible to take exact account of the vortex configurations by means of a dual transformation[29]. One can extract the contribution from the multivalued configuration by means of the decomposition $\theta(x) = \theta'(x) + \tilde{\theta}(x)$, where $\oint_C \nabla\theta' = 0$ and $\oint_C \nabla\tilde{\theta} = 2\pi m_i \neq 0$. Substituting this into Eq. (3), one can show that the vortex part of the XY Hamiltonian in $2d$ is equivalent to a Coulomb gas[30] with charges playing the role of vortices. More precisely, it is the Villain model that can be exactly mapped onto the Coulomb gas, and spin-wave–vortex interactions give rise to additional contributions that can be computed. In absence of a magnetic field, the mapping leads to a neutral Coulomb gas with $\sum_i m_i = 0$. The Coulomb gas formalism allows for a sensible low temperature expansion, indeed for $T \leq T_{\mathrm{BKT}}$ we expect only singly charged vortices to be relevant and we thus include only $m_i = \pm 1$ configurations. The latter give rise to an additional cosine potential in the spin-wave Hamiltonian, and the duality transformation maps this to the SG model in the dual phase field Φ,

$$S_{SG}[\Phi] = \int d^2x \left(\frac{1}{2}\partial_\mu\Phi\partial_\mu\Phi - u\cos(\beta\Phi)\right), \tag{8}$$

with dimensional coupling u and dimensionless SG coupling β (not to be confused with the symbol $\beta = 1/T$). Also the XY model can be mapped onto the SG model (8) via the Coulomb gas[29]; this can be intuitively understood because the compact nature of the variable θ allows only perturbations in the form of a periodic operator. Thus, from the RG point of view the theory space of a periodic field θ is naturally described, at least at lowest order, by the SG model[76]. Note, however, that the original compact phase θ is replaced by the dual phase Φ in the SG model. We also observe that the mapping between the XY and the SG model[29,37,74] has the advantage to give an explicit form for the bare coupling of the SG model.

A key point, which we will use in the following, is that the spin-wave Hamiltonian (3) with a *compact* variable θ is equivalent to the Villain model, which, once vortices with $|m_i| > 1$ are neglected, is dual to the SG model (8) with $\beta^2 = 4\pi^2 K$.

The SG model has also been studied extensively in the FRG framework, which provides a nonperturbative generalization of the original Kosterlitz-Thouless RG equations[34,52,77–81]. In the following, after briefly reviewing in Section II B previous FRG work for the $O(2)$ model, we will combine the AP parametrization of the FRG with the SG results into a comprehensive FRG treatment including amplitude, spin-wave and vortex excitations.

B. FRG results for the $O(2)$ model in $2d$

In this section we review and discuss previous FRG results for the $O(N = 2)$ field theory in $d = 2$. One can write the quartic potential with $\rho = |\varphi|^2$ as

$$U(\rho) = \frac{\lambda_k}{2}(\rho - \kappa_k)^2 \tag{9}$$

and derive FRG equations for the flow of the scale-dependent couplings. In the LPA′ approximation[39] one has

$$\partial_t \tilde{\lambda}_k = (2-2\eta_k)\tilde{\lambda}_k - \tilde{\lambda}_k^2 \frac{(4-\eta_k)}{8\pi}\left(N-1+\frac{1}{(1+2\tilde{\kappa}_k\tilde{\lambda}_k)^3}\right), \tag{10}$$

where $k \propto L^{-1}$ is an infrared momentum cutoff, $\tilde{\lambda}_k = k^{d-4}\lambda_k$ and $t = -\log(ka) = 0\ldots\infty$ is the RG "time". The flow equation for $\tilde{\kappa}_k$ reads

$$\partial_t \tilde{\kappa}_k = \eta_k\tilde{\kappa}_k - \frac{(4-\eta_k)}{16\pi}\left(N-1+\frac{1}{(1+2\tilde{\kappa}_k\tilde{\lambda}_k)^2}\right), \tag{11}$$

with $\tilde{\kappa}_k = k^{2-d}\kappa_k = \kappa_k$. The anomalous dimension at scale k is given by

$$\eta_k = \frac{1}{\pi}\frac{\tilde{\kappa}_k\tilde{\lambda}_k^2}{(1+2\tilde{\kappa}_k\tilde{\lambda}_k)^2}. \tag{12}$$

These flow equations for $\tilde{\lambda}_k$ and $\tilde{\kappa}_k$ may easily be integrated numerically[49], and the resulting phase diagram is shown in Fig. 1. For initial conditions with sufficiently large $\tilde{\kappa}_k$ the flow is rapidly attracted to a line of pseudo-fixed points at an almost constant value of $\tilde{\lambda}_k$. Once this line is reached, the flow slows down substantially and leaves the system in its symmetry broken phase for intermediate RG times. For larger $t \to \infty$ the flow eventually escapes the low-temperature phase and reaches the high-temperature phase with $\tilde{\kappa}_k = 0$ at a finite time $t < \infty$.

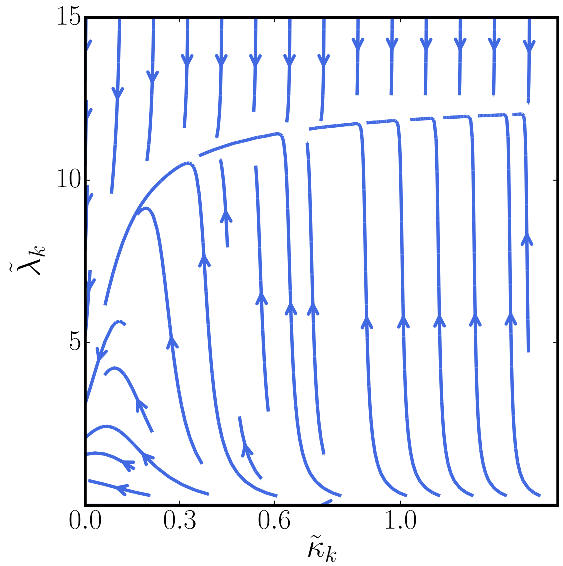

FIG. 1. Flow diagram of the $O(2)$ symmetric $|\varphi|^4$ theory with flowing effective potential (9) in parametrization (i). The flow is first attracted toward a line of pseudo-fixed points at large $\tilde{\kappa}_k$; then the flow proceeds very slowly along this line toward $(\tilde{\kappa}_k, \tilde{\lambda}_k) = (0,0)$, which corresponds to the high-temperature phase.

Following[49], one can identify the unstable pseudo-fixed line at finite $\tilde{\lambda}_k$ with the low-temperature phase of the BKT transition. In this symmetry broken phase, the complex field can be decomposed into radial and transverse modes. The radial (or massive) mode ρ is effectively frozen by its finite mass $m_m \propto 2\tilde{\lambda}_k\tilde{\kappa}_k$, while the remaining massless Goldstone mode ($m_g = 0$) is effectively described by the spin-wave Hamiltonian (3) and has algebraic correlations. On the other hand, for initial conditions in the small $\tilde{\kappa}_k$ region, the flow is rapidly attracted to the point $\tilde{\kappa}_k = \tilde{\lambda}_k = 0$ and enters a high-temperature $U(1)$ symmetric phase with exponential correlations, which is identified with the disordered, high-temperature phase of the BKT transition.

It is remarkable that the FRG treatment of the $O(2)$ model is able to recover the high-temperature phase without explicitly considering vortex configurations. Indeed, the complex field parametrization (i) implicitly includes the comparct phase variable responsible for vortex excitations, in contrast to the spin-wave action (3) when the phase is considered non-periodic.

On the other hand, in the thermodynamic limit $k \to 0$ there is only one regime in Fig. 1, showing that spin-wave excitations are always massive in this approximation. More precisely, the FRG flow presented in Fig. 1 does not exhibit a sharp BKT transition but rather a smooth crossover. Indeed, for large enough length scales $k^{-1} \gg a$ the flow always reaches the symmetric phase and algebraic correlations disappear in the thermodynamic limit for any $T > 0$. This is the result of vortex unbinding, hence the FRG calculation[49] overestimates the effect of vortex configurations which appear to be relevant at any finite temperature.

It is useful to observe that a similar behavior was already found in the Migdal approach to the XY model[29]. There, the RG equations are written in terms of the periodic potential $V(\theta)$ between the phases of two neighboring spins. Even in that scheme an unstable pseudo-fixed line is found with a phase potential very similar to the one of the Villain model[28]. On the other hand, for small enough values of k the interaction potential always reaches a high-temperature fixed point.

The failure of the Migdal approximation to reproduce the expected low-energy physics of the $2d$ XY model has been attributed to an insufficient representation of vortex correlations, which leads to a systematic overestimation of the vortex contribution in the long-wavelength limit[29]. A similar effect may be responsible for the picture found in the lowest-order FRG truncation. Indeed, neglecting higher derivative terms in the $|\varphi|^4$ action may overestimate the effect of vortex degrees of freedom in the thermodynamic limit. Nevertheless, it is an open question whether fully including higher derivatives reproduces vortex-vortex correlations with the correct power-law decay to stabilize the low-temperature phase.

One way to extract an anomalous dimension from the LPA′ FRG treatment with complex field parametriza-

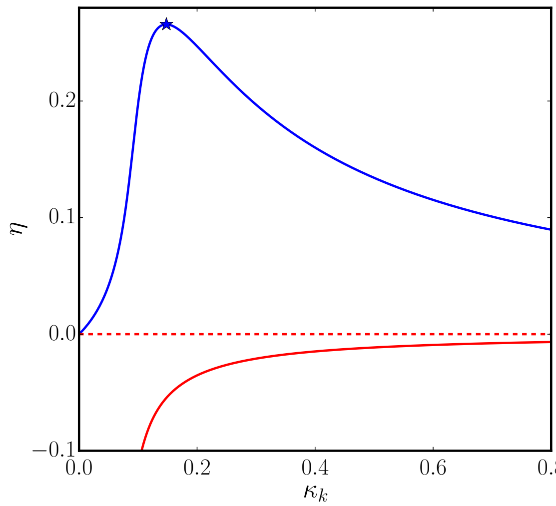

FIG. 2. The anomalous dimension η in the $O(2)$ model (blue solid line) represents the power-law decay of the two-point correlation function. Its value is found from Eq. (12) along the pseudo-fixed line in Fig. 1. The star represents the choice of η in[49] and[54]. The lower, red solid curve gives the values of $\partial_t\tilde{\kappa}_k$ along the same pseudo-fixed line, while a line of true fixed points would have $\partial_t\tilde{\kappa}_k = 0$, as one has in[54] by a temperature-dependent choice of the cutoff function.

tion (i) is to effectively discard the finite flow along the pseudo-fixed line. The condition $\partial_t\tilde{\lambda}_k = 0$ is evaluated numerically to obtain a curve $\tilde{\lambda}_k = f(\tilde{\kappa}_k)$ in $(\tilde{\kappa}_k, \tilde{\lambda}_k)$ space. Once the finite flow $\partial_t\tilde{\kappa}_k$ is discarded along this line, one may compute the power-law exponent η of the correlation function in the thermodynamic limit using Eq. (12).

The result for η along the line of pseudo-fixed points is depicted as a blue line in Fig. 2. The red curve below shows the residual flow $\partial_t\tilde{\kappa}_k$ along the pseudo-fixed line. This flow should vanish for a line of true fixed points, while as it can be seen in in Fig. 2 it vanishes only in the limit $\tilde{\kappa}_k \to \infty$, remaining finite for smaller $\tilde{\kappa}_k$. Nevertheless, it is possible to identify a point where $|\partial_t\tilde{\kappa}_k|$ starts to increase sharply and drives the system to the disorder phase for small scales k. The anomalous dimension at the turning point is surprisingly close to the expected value 1/4. In the Sections IV–V below we show how a line of *true* fixed points and gapped amplitude excitations are found with the AP parametrization. As a basis for this, we first discuss the mapping between the XY and $|\varphi|^4$ models in Section III.

III. MAPPING OF THE MODELS

In this section we derive the explicit mapping of the XY model into a suitable $|\varphi|^4$ theory via a Hubbard-Stratonovich transformation[6,53,82]. While this mapping is well known, we present it briefly in order to demonstrate how the XY model of unitary spins is equivalent to a complex field φ with density fluctuations. Via the mapping, our subsequent FRG analysis of the $|\varphi|^4$ model applies also to the XY model.

Our starting point is the XY model (1), which can be written (apart from a constant energy) as

$$H_{XY} = -J\sum_{\langle ij\rangle}\left(s_{x,i}s_{x,j} + s_{y,i}s_{y,j}\right), \tag{13}$$

where $s_{x,i} \equiv \cos\theta_i$, $s_{y,i} \equiv \sin\theta_i$ can be combined into a vector $\boldsymbol{s}_i = (s_{x,i}, s_{y,i})$ with $\boldsymbol{s}_i^2 = 1$. The partition function is then given by

$$Z(\beta) = \int \mathcal{D}s\, e^{\beta J\sum_{\langle ij\rangle}(s_{x,i}s_{x,j}+s_{y,i}s_{y,j})}\Pi_j\delta\left(\boldsymbol{s}_j^2 - 1\right) \tag{14}$$

with $Ds = \Pi_i ds_{x,i}ds_{y,i} \equiv \Pi_i d\boldsymbol{s}_i$. One can rewrite the partition function in the form

$$Z(\beta) = \int \mathcal{D}s\, e^{\boldsymbol{s}\cdot\frac{K'}{2}\cdot\boldsymbol{s}}\Pi_j\delta\left(\boldsymbol{s}_j^2 - 1\right) \tag{15}$$

where $\boldsymbol{s} = (s_{x,1}, s_{y,1}, \cdots, s_{x,N}, s_{y,N})$ is a $2N$-dimensional vector and the matrix K' has elements $2\beta J$ on the neighboring upper and lower diagonals. To perform the Hubbard-Stratonovich transformation we use the Gaussian identity

$$e^{\boldsymbol{s}\cdot\frac{K'}{2}\cdot\boldsymbol{s}} = \left[(2\pi)^N\sqrt{\det K'}\right]^{-1}\int \mathcal{D}\phi\, e^{-\boldsymbol{\phi}\cdot\frac{K'^{-1}}{2}\cdot\boldsymbol{\phi} - \boldsymbol{s}\cdot\boldsymbol{\phi}} \tag{16}$$

where $\boldsymbol{\phi}$ is a $2N$ vector composed of N two-component vectors $\boldsymbol{\phi}_j$. Since K' is not positive definite, we replace it by a shifted interaction

$$K = K' + 2\beta\mu\,\mathbb{I} \tag{17}$$

that is positive definite for an appropriately chosen constant μ; this amounts to a redefinition of the zero point energy of the system. We then obtain

$$Z(\beta) = \left[(2\pi)^N\sqrt{\det K}\right]^{-1}\int \mathcal{D}\phi\, e^{-\boldsymbol{\phi}\cdot\frac{K^{-1}}{2}\cdot\boldsymbol{\phi} + \sum_j U(\boldsymbol{\phi}_j)}, \tag{18}$$

where the potential U is defined by

$$e^{U(\boldsymbol{\phi}_j)} = \int d\boldsymbol{s}_j\, e^{-\boldsymbol{s}_j\cdot\boldsymbol{\phi}_j}\,\delta\left(\boldsymbol{s}_j^2 - 1\right). \tag{19}$$

U can depend only on the quadratic invariant $\rho_j = \phi_{x,j}^2 + \phi_{y,j}^2$, and we obtain

$$U(\boldsymbol{\phi}) = \log\left(\pi I_0(\sqrt{\rho})\right) \tag{20}$$

in terms of the modified Bessel function I_0. The matrix K^{-1} is diagonal in Fourier space with entries

$$K(q) = 2\beta(\mu + J\varepsilon_0(q)) \tag{21}$$

where

$$\varepsilon_0(q) = \sum_{\nu=1}^{d} \cos(q_\nu a) \tag{22}$$

is the dispersion relation on a d-dimensional cubic lattice for momentum components q_ν and lattice spacing a (in our case $d = 2$). It will be convenient to shift the kinetic term as

$$S_{\rm kin}[\phi] = \frac{1}{2}\sum_q \phi_q \left(\frac{1}{K(q)} - \frac{1}{K(0)}\right)\phi_{-q}. \tag{23}$$

After a field rescaling

$$\phi \to 2\sqrt{\frac{\beta}{J}}(Jd+\mu)\varphi \tag{24}$$

one obtains the kinetic term

$$S_{\rm kin}[\varphi] = \frac{1}{2}\sum_q \varphi_q \varepsilon(q)\varphi_{-q}. \tag{25}$$

with dispersion relation[53]

$$\varepsilon(q) = 2(Jd+\mu)\frac{d-\varepsilon_0(q)}{J\varepsilon_0(q)+\mu}. \tag{26}$$

In the continuum limit $a \to 0$ we recover

$$\varepsilon_{\rm cl}(q) = q^2 \tag{27}$$

to lowest order in q, where the subscript cl stands for continuum limit. The potential term in the rescaled field reads

$$S_{\rm pot}[\varphi] = \int d^dx \left[-U\left(2\sqrt{\frac{\beta}{J}}(Jd+\mu)\varphi\right) + \frac{Jd+\mu}{J}|\varphi|^2\right]. \tag{28}$$

With this mapping of the XY model into a $|\varphi|^4$ theory, we can subsequently use our functional RG equations for both models; only the the initial conditions, *i.e.*, the functional forms of the dispersion $\varepsilon(q)$ and the potential $U(\rho)$, are different and discriminate between the microscopic XY and $|\varphi|^4$ models. We finally observe that in the XY model there are not, by construction, amplitude fluctuations, but there are spin-wave excitations, which are seen as (strongly) gapped amplitude fluctuations in the action (28).

IV. THE AMPLITUDE-PHASE PARAMETRIZATION

The complex field φ can be parametrized in terms of real amplitude ρ and phase θ as

$$\varphi(x) = \sqrt{\rho(x)}e^{i\theta(x)}. \tag{29}$$

In this AP parametrization (iii) the $|\varphi|^4$ action (2) reads

$$S[\varphi] = \int d^dx \left\{\frac{1}{8\rho}\partial_\mu\rho\partial_\mu\rho + \frac{\rho}{2}\partial_\mu\theta\partial_\mu\theta + U(\rho)\right\}. \tag{30}$$

When applied to the XY model with the mapping (28), the field expectation value is related to the XY magnetization by $\langle\varphi\rangle = \sqrt{\beta J}m$.

Perturbative arguments suggest that the amplitude mode is always gapped and does not influence the critical behavior[55,63]. Instead, the critical behavior is dominated by massless phase fluctuations. In $d = 2$, only single vertex diagrams are relevant[27], and since the perturbative expansion for the phase correlation function does not contain any single vertex diagram, we expect only a finite renormalization of the superfluid stiffness in the action (30). In the following we will explicitly treat amplitude fluctuation effects to show how, even in the nonperturbative picture, they remain gapped at criticality.

As a preliminary step, we first discuss uncoupled amplitude and phase fluctuations. In this case, the superfluid stiffness $\rho = \kappa_k$ in the phase kinetic term remains fixed at the minimum of the potential $U(\rho)$. The total action (30) then decouples into a sum of two actions

$$S[\varphi] \simeq S_A[\rho] + S_P[\theta] \tag{31}$$

where

$$S_A[\rho] = \int d^2x \left\{\frac{1}{8\rho}\partial_\mu\rho\partial_\mu\rho + U(\rho)\right\}, \tag{32}$$

$$S_P[\theta] = \frac{\kappa_k}{2}\int d^2x\, \partial_\mu\theta\partial_\mu\theta. \tag{33}$$

The phase action (33) is equivalent to spin-wave model (3) with $K = \kappa_k$, while for the XY model it is $K = \kappa_k\beta J$. If one considers the phase variable θ in (33) as noncompact, the correlation function $\langle e^{i[\theta(x)-\theta(y)]}\rangle$ is algebraic[14] and no regularization is necessary to obtain this behavior[55]. However, in order to obtain the high-temperature phase by vortex unbinding one needs to treat the phase as periodic and regularization is necessary. The periodic phase action (33) [or (3)] maps into the SG model (8) with $\beta^2 = \kappa_k$.

The treatment within the AP parametrization shows that the low-temperature expansion of the $|\varphi|^4$ and XY models must coincide, at least as long as perturbative arguments are correct and amplitude fluctuations do not influence the thermodynamic behavior. However, it is worth noting that this analysis still does not yield a conclusive picture. Indeed, while the previous FRG analysis based on the $|\varphi|^4$ action (2) leads to a finite correlation length at any temperature and reproduces the BKT behavior only as a crossover, the amplitude and phase scheme is equivalent to the spin-wave approximation of the XY model and yields algebraic correlation at any temperature, $T_{\rm BKT} = \infty$.

To complete the picture, it is therefore necessary to introduce vortex configurations. The spin-wave analysis in Appendix A does not include discontinuous configurations of the field θ and perturbative arguments cannot account for topological excitations. These can be included using the dual mapping described in[29,74] or by explicitly introducing singular phase configurations[37,83]. The total partition function of the system is then given by

$$Z \simeq Z_A Z_P, \tag{34}$$

where we used the decomposition in Eq. (31).

In the case of frozen amplitude fluctuations, this model becomes a pure phase SG model with a line of fixed points and is described by the BKT flow equations

$$\partial_t K_k = -\pi g_k^2 K_k^2, \tag{35}$$

$$\partial_t g_k = \pi \left(\frac{2}{\pi} - K_k \right) g_k \tag{36}$$

where K is the superfluid (phase) stiffness and g_k is the vortex fugacity. The fugacity g is related to the SG parameter as $u = g/\pi$.

At the bare level, K and g assume the values

$$K_\Lambda = \rho_0, \tag{37}$$

$$g_\Lambda = 2\pi e^{-\pi^2 K_\Lambda/2} \tag{38}$$

for the $|\varphi|^4$ model, and

$$K_\Lambda = \beta J, \tag{39}$$

$$g_\Lambda = 2\pi e^{-\pi^2 K_\Lambda/2} \tag{40}$$

for the XY model. Note that Eqs. (37)–(40) are exact in the Villain approximation of both models, but represent only the lowest-order approximation in their temperature expansions.

In the small vortex fugacity limit $g_k \ll 1$ the BKT flow Eqs. (35) and (36) reproduce the BKT temperature in Eq. (6), while for larger values of the initial condition g_Λ the BKT flow introduces multi-vortex corrections which lower the BKT temperature. For a discussion of these effects and of vortex core energies we refer to[72,84]; the prediction for the jump of the superfluid stiffness, $\frac{2mT}{\pi}\left(1 - 16\pi e^{-4\pi}\right)$ with a correction of 0.02% with respect to the Nelson-Kosterlitz prediction $2mT/\pi$, has been tested in extensive Monte Carlo simulations[72,73].

V. RESULTS

Although the universal behavior of the BKT transition is completely driven by topological excitations, in the $|\varphi|^4$ and XY models the contribution of, respectively, longitudinal and amplitude fluctuations to non-universal quantities may be different. Due to the mapping discussed in Section III, it is possible to build a $|\varphi|^4$ model which exactly reproduces the XY model and where the role of longitudinal spin excitations is played by amplitude fluctuations. It is then convenient to study the BKT transition first in the $|\varphi|^4$ formalism and then transfer the results to the XY model, which we do subsequently in the two next Sections V A and V B.

A. $|\varphi|^4$ model

In this section we apply the FRG to the $|\varphi|^4$ action in the AP parametrization (30). As discussed in the previous section, at the perturbative level the amplitude mode ρ remains gapped while the phase fluctuations θ produce power-law correlations at any finite temperature, so the high-temperature phase of the BKT transition is not reproduced. In this section we revisit this issue at the non-pertubative level.

Our FRG procedure is based on two steps: *(a)* we first perform the FRG flow for the amplitude part S_A of the action (32), which yields a renormalized superfluid stiffness; *(b)* we then insert this stiffness into the phase part S_P of the action (33), which for a compact phase is equivalent to the SG model (8) so we can use the BKT flow Eqs (35)–(36).

In the FRG approach for the amplitude part we introduce as infrared regulator a momentum dependent mass term for the amplitude fluctuations. As the cutoff scale is lowered, the effective action flows from the model-dependent initial condition (32) to the full effective action. For the flowing effective action we choose the ansatz

$$\Gamma_k[\rho,\theta] = \int d^d x \left\{ \frac{1}{8\rho} \partial_\mu \rho \partial_\mu \rho + \frac{\rho}{2} \partial_\mu \theta \partial_\mu \theta + U_k(\rho) \right\}, \tag{41}$$

and with the regulator (B2) we obtain the flow Eq. (B4) for the effective potential of amplitude and phase fluctuations, for details see Appendix B.

The flow equation is solved numerically for the full potential $U_k(\rho)$. In order to draw a flow diagram, we Taylor expand the potential $U_k = \lambda_k(\rho - \kappa_k)^2/2$ around its minimum $\rho = \kappa_k$ for every k and trace the flow in (κ_k, λ_k) space. The resulting flow diagram is shown in the left Fig. 3(a) in terms of the rescaled "dimensionless" couplings $\tilde{\lambda}_k = k^{d-4}\lambda_k$ and $\tilde{\kappa}_k = k^{2-d}\kappa_k$. This first naive attempt at the AP flow is not yet correct: indeed in the lower left corner of the phase diagram the λ_k coupling becomes irrelevant and the flow runs toward a region of gapless amplitude fluctuations; although this effect is not as severe as in previous parametrization, since it arises only for small values of the bare coupling λ_Λ, it is not in agreement with the expectation of irrelevant amplitude fluctuations in the thermodynamic limit. This inconsistency arises from an IR divergent term in the standard formulation of the Wetterich equation. Indeed, already the flow of the free Gaussian model in the AP parametrization has the same divergence because the phase kinetic term depends on the field ρ.

A simple way to avoid this unphysical divergence is to subtract the contribution of the Gaussian theory from the Wetterich equation, following standard procedure in free energy calculations. With this modification the potential

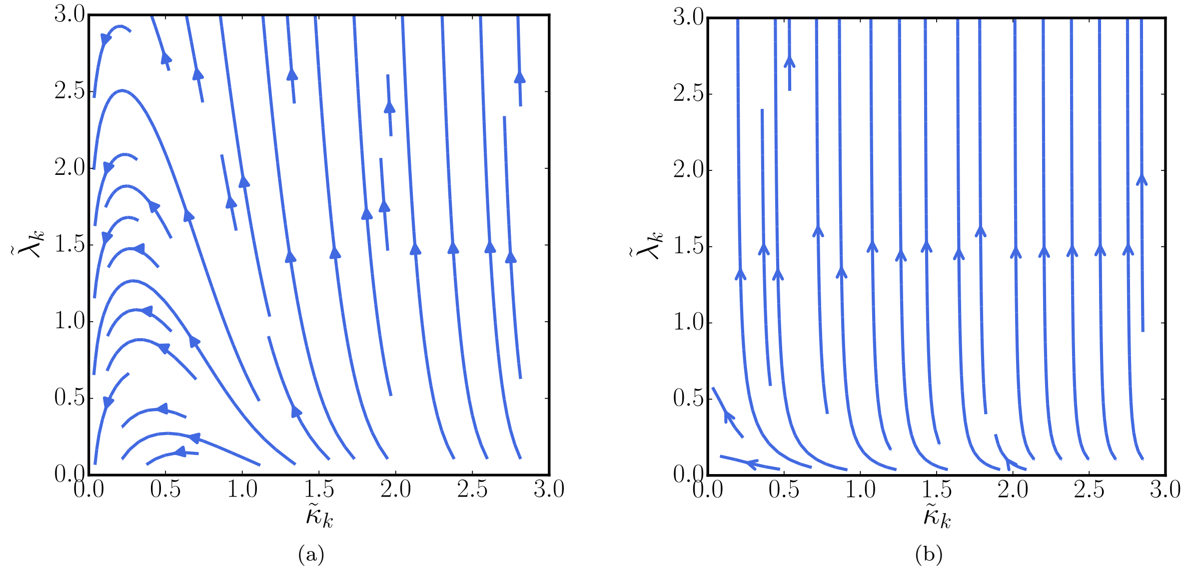

FIG. 3. Flow diagram for the rescaled superfluid stiffness $\tilde{\kappa}_k$ and interaction $\tilde{\lambda}_k$ due to amplitude fluctuations in $d = 2$. For large enough $\tilde{\lambda}_\Lambda$ the flow always proceeds towards an infinitely interacting $\tilde{\lambda}_{k\simeq 0} \simeq +\infty$ fixed line where the expectation value $\tilde{\rho}_0 = \kappa_k$ is effectively frozen. **(a)** The naive AP flow is (uncorrectly) attracted for $\tilde{\lambda}_\Lambda \ll 1$ toward the free theory. **(b)** The modified AP flow with the Gaussian contributions subtracted reproduces the expected flow diagram.

flow equation (B4) becomes

$$\partial_t U_k(\rho) = \frac{4\alpha\rho k^2 \log\left(\frac{\alpha + 4\alpha\rho U^{(2)}(\rho)/k^2}{\alpha + U^{(2)}(\rho)/k^2}\right)}{4\pi(4\alpha\rho - 1)}. \tag{42}$$

Note that phase fluctuations do not contribute to the flow of the potential in this simplest FRG truncation. The parameter $\alpha = \alpha_\rho$ characterizes the regulator (B2); Fig. 3 has been plotted with $\alpha_\rho = 2$, but below we set $\alpha = (4\kappa_*)^{-1}$ self-consistently with the value of κ at the end of the flow.

The modified Eq. (42) now produces the correct flow diagram shown in the right Fig. 3(b). As expected, the mass term of amplitude fluctuations does not vanish. The dimensionless $\tilde{\lambda}_k$ keeps growing because the action (41) with a noncompact phase has no fixed point. Indeed, $\tilde{\kappa}_k$ is marginal in $2d$, and after an initial renormalization by amplitude fluctuations at finite $\tilde{\lambda}_k$, it remains frozen up to infinite length scales ($k \to 0$).

The results of Fig. 3(b) are in agreement with the expectation of perturbation theory and show that amplitude fluctuations are irrelevant in the RG sense and lead to a finite renormalization of the stiffness. It is useful to compare the results of Figs. 1 and 3(a) with those of Fig. 3(b): both represent the theory space of a $2d$ two-component field theory where the order parameter has $U(1)$ symmetry. However, differences arise in the treatment of the kinetic term: in Fig. 1 the flow for the couplings has been obtained including the full $|\varphi|^4$ invariant kinetic term, which incorporates both amplitude and phase degrees of freedom. There, for λ_Λ large enough, the flow is attracted to a pseudo-fixed line and the IR theory appears to have finite $\tilde{\kappa}_k$, finite $\tilde{\lambda}_k$ and massive amplitude fluctuations at finite k. At the same time, a fixed $\tilde{\lambda}_k$ produces a vanishing dimensionful $\lambda_k = k^2\tilde{\lambda}_k$ in the thermodynamic limit $k \to 0$. Hence, it is not surprising that for k small enough the superfluid density κ_k tends to vanish because of the increasing relevance of amplitude fluctuations. In contrast, the modified flow in the right Fig. 3(b) is consistent with fully gapped amplitude fluctuation and frozen amplitude (superfluid stiffness) $\kappa_k \equiv \kappa_*$. Indeed, for every finite $\tilde{\lambda}_\Lambda > 0$ the flow is attracted by a stream line at fixed $\tilde{\kappa}_k$ and $\tilde{\lambda}_k \propto k^{-2}\lambda_*$, yielding $\lambda_k \simeq \lambda_*$ for $k \ll \Lambda$.

Having shown that the modified AP flow agrees with the perturbative results and the BKT scenario, we are in a position to verify that our approach based reproduces the expected universality of the thermodynamics of the $2d$ Bose gas[59,60,62–65] and to quantify the agreement with Monte-Carlo results. In particular, starting the flow from the initial conditions (37) we can compute:

a. the superfluid density ρ_s, which is equal to the coupling κ_*; and

b. the critical chemical potential μ_c as a function of the bare interaction U.

To achieve this result we perform the renormalization group procedure described above with the initial condition

$$U_\Lambda(\rho) = \frac{U}{2}(\rho - \kappa_\Lambda)^2, \tag{43}$$

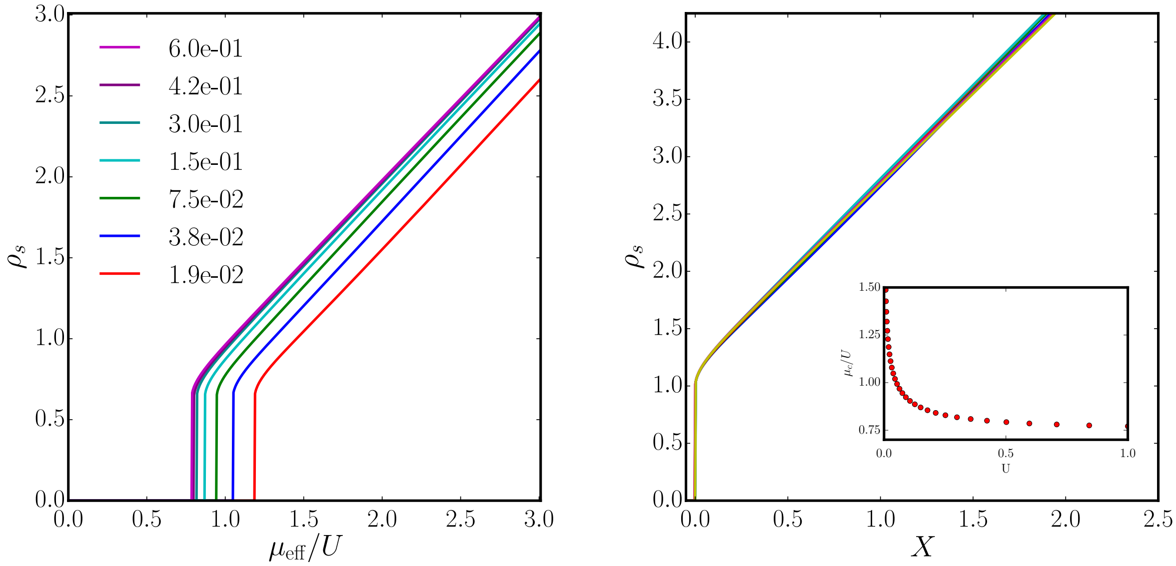

(a) (b)

FIG. 4. Superfluid density ρ_s as a function of chemical potential. **(a)** ρ_s/mT *vs* μ/U for 7 different values of $U = 1 \ldots 0.02$ from top to bottom. **(b)** ρ_s/mT *vs* dimensionless chemical potential X. **Inset:** Critical chemical potential μ_c/U *vs* U.

where U is the effective interaction and $\mu = U\kappa_\Lambda$ is the chemical potential of the classical $2d$ $|\varphi|^4$ model we are studying.

The known results for the $2d$ quantum Bose gas with which we want to compare are the following:

1) the thermodynamic quantities have to collapse once expressed in terms of the dimensionless variable

$$X = \frac{\mu - \mu_c}{mTU}, \tag{44}$$

which measures the distance from the critical point.

2) The superfluid density defines a function $f(X)$ via the relation

$$\rho_s = \frac{2mT}{\pi} f(X). \tag{45}$$

Note that the predicted jump of the superfluid stiffness $\rho_s = 2mT/\pi$ at criticality[21] implies that $f(X)$ jumps from 0 to 1 at $X = 0$. The collapse of the superfluidity function using the variable X is shown in Figs. 4(a)-4(b).

3) for small $X > 0$ one has

$$f(X) = 1 + \sqrt{2\kappa' X}, \tag{46}$$

with coefficient[60]

$$\kappa' = 0.61 \pm 0.01. \tag{47}$$

4) For $2d$ quantum systems in the continuum, one has the following results in the weakly interacting limit for the critical density ρ_c and the critical chemical potential μ_c (respectively in the canonical and grand-canonical ensembles):

$$n_c = \frac{mT}{2\pi} \ln \frac{\xi}{mU}, \tag{48}$$

$$\mu_c = \frac{mTU}{\pi} \ln \frac{\xi_\mu}{mU}. \tag{49}$$

The parameters ξ, ξ_μ, extracted from Monte Carlo simulations in a classical lattice $|\varphi|^4$ model and via a careful analysis of the mapping between the simulated lattice model and the continuum limits, have been estimated to be $\xi = 380 \pm 3$, $\xi_\mu = 13.2 \pm 0.4$[59,60]. The logarithm of their ratio,

$$\theta_0 \equiv \frac{1}{\pi} \ln{(\xi/\xi_\mu)}, \tag{50}$$

is a non-trivial universal number, determined to be[60]

$$\theta_0 = 1.068 \pm 0.01. \tag{51}$$

We now present our results for these non-universal and universal properties of the $|\varphi|^4$ model. In Fig. 4(a) we report our results for the superfluid fraction ρ_s for different values of U. In Fig. 4(b) we plot the same curves vs the dimensionless variable X. We find that they collapse almost perfectly even for a wide range of interactions $U = 0.02, \ldots, 0.6$. Note that the spreading between the curves increases for large X, as expected, since the

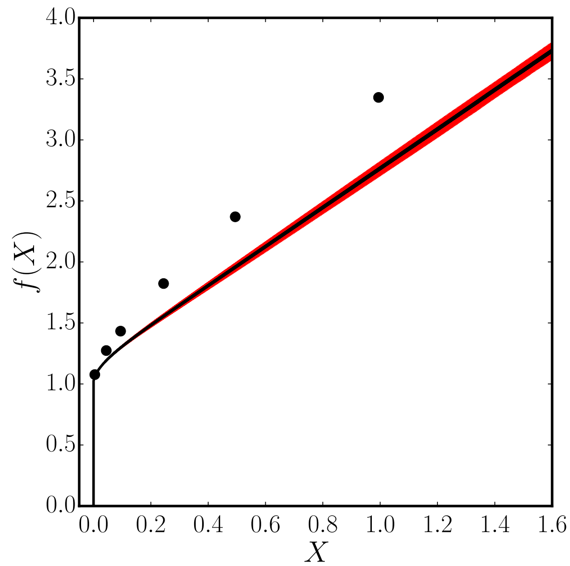

FIG. 5. (a) Superfluid scaling function $f(X) = \pi\rho_s/2mT$ (black line) as a function of the chemical potential variable X (average and variance over 30 sets of data for different interaction values U), the standard deviation is shown as a red shadow. Black dots are the MC data from[60].

universality should hold only in the fluctuation regime up to $X \approx 1/mU$ and we use also rather large values of U. To quantitatively determine the function $f(X)$ we perform an interpolation of the curves for $\rho_s(X)$, some of them shown in Fig. 4(b), and compute their average and variance, which are reported in Fig. 5. The average has been computed over a total number of 30 curves obtained for 30 different values of the interaction logarithmically spaced in the interval $U \in [0, 1]$, the curve $f(X)$ can be trusted also for large X since the statistical weight of large interaction $U > 0.5$ is small. Agreement with Monte Carlo data[60] is rather good, also considering that we are using the lowest order perturbative SG results (37)–(38).

Our findings for μ_c as a function of U are given in the inset of Fig. 4(b). Logarithmic corrections to the relation $\mu_c \propto U$ are found, in agreement with Eq. (49). The coefficient ξ_μ entering such logarithmic corrections is not reported since the fitting procedure employed was not robust enough and the result strongly depends on the range of interactions considered, even for $U \leq 0.3$ which should be within the range of validity of Eq. (49)[85].

The $\rho_s(X)$ in Fig. 4(b) determines the function $f(X) = \pi\rho_s(X)/2mT$ reported in Fig. 5. From $f(X)$ we can obtain estimates for the universal quantities κ' and θ_0. Fitting with expression Eq. (46), the data in Fig. 5 yield

$$\kappa'_{(\mathrm{FRG})} = 0.67 \pm 0.07, \tag{52}$$

in reasonably good agreement with the Monte Carlo result (47). The latter result has been obtained from a linear fit of the curves in Fig. 4(a) and averaging κ' over the values obtained for different interactions. The average is consistent with (52) while the error is partly due to difficulties in fitting procedure close to the transition point and partially to non-perfect universality of the curves in Fig. 4(a).

Regarding θ_0, we observe that for relatively large X one has $f(X) \approx (\pi/2)\theta(X) - 1/4$ in terms of the universal equation of state $\theta(X)$[60]. It should be noted that in order to evaluate $\theta_0 = \theta(X = 0)$ from $f(X)$ one shall extrapolate the value of a curve obtained for large X to the point $X = 0$. Such extrapolation has been done assuming polynomial behavior of $\theta(X)$. A polynomial fit of the ρ_s curves of different interactions at high values of X yields

$$\theta_{0(\mathrm{FRG})} = 1.033 \pm 0.032, \tag{53}$$

again in fairly good agreement with the Monte Carlo result (51).

B. *XY* model

As we discussed in Sections III–IV, one can treat the XY model as a $|\varphi|^4$ model, provided that one uses the appropriate initial condition for the RG flow, as extracted from the mapping of Section III, and that one rescales the field by $\sqrt{\beta J}$ to have a magnetization with absolute value smaller than one.

The XY model has been the subject of intense investigations from different perspectives and several quantities have been studied in detail, which we can now study with the FRG approach presented in this paper. Here, to test the validity of our approach, we focus on the renormalized phase (superfluid) stiffness $J_s(T)$ and quantify the effect of amplitude fluctuations on it. We proceed by computing κ_* as discussed in the previous Section V A, then the stiffness is given by

$$J_s(T) = J\kappa_*. \tag{54}$$

All the physical quantities should be independent of the mapping parameter μ[53]. However, in the following we are going to discard lattice effects, effectively replacing the lattice dispersion (26) with the continuum dispersion (28). Such an approximation introduces a μ dependence in the physical quantities, which we may fix either from mean-field or low-temperature results.

To clarify the different approximations which we are going to consider for the FRG computation of $J_s(T)$, let us recapitulate the logic followed so far. Starting from the action of the $|\varphi|^4$ model in the continuum limit, we introduced the AP parametrization (29) and we decoupled the phase and amplitude degrees of freedom by substituting $\rho = \kappa_k$ into the phase kinetic term. The phase action (33) is then equivalent to the low-temperature expression of the XY Hamiltonian (3) and we can apply the usual BKT flow Eqs. (35) and (36). The amplitude fluctuations then encode all fluctuations except for vortices, which are encoded at perturbative level in the BKT flow equations.

It is instructive to consider first the mean-field approximation. A first step is to completely discard amplitude fluctuation and simply set $\kappa_k = \text{const}$, which can be reabsorbed into the definition of J. A further step is to consider only a saddle point approximation for the amplitude fluctuations. Their expectation value is given by $\kappa_{MF} = \rho_{\rm MF}(T)$ such that

$$\frac{\partial S_{\rm pot}[\sqrt{\beta J \rho_{\rm MF}}]}{\partial \rho_{\rm MF}} = 0, \tag{55}$$

where $S_{\rm pot}[\varphi]$ is defined in Eq. (28) and the additional $\sqrt{\beta J}$ factor in the argument is needed to reproduce the $K \equiv \beta J$ factor in Eq. (3). Thus, at first order in our treatment we find

$$J_s(T) \equiv J \kappa_{\rm MF}(T). \tag{56}$$

For small T, longitudinal fluctuation are practically frozen and $\lim_{T\to 0} J_s(T) = J$. At larger temperatures $\kappa_{\rm MF}(T)$ decreases since longitudinal fluctuations reduce the stiffness. Finally, $J_s(T)$ vanishes at a finite temperature value $T_{\rm MF} > T_{\rm BKT}$. The mean-field critical temperature $T_{\rm MF}$ is given by $T_{\rm MF} = 2J$ ($T_{\rm MF} = dJ$ for a hypercubic lattice in d dimensions). To obtain this value of $T_{\rm MF}$ one has to fix $\mu = 0$. This choice turns out to be a reasonable one, since one finds for small T

$$\frac{J_s(T)}{J} = 1 - \frac{T}{2T_{\rm MF}} + \cdots = 1 - \frac{T}{4J} + \cdots, \tag{57}$$

in agreement with the results of the self-consistent harmonic approximation[86], which predicts $J_s(T)/J = 1 - T/zJ$ for a model with z nearest neighbors at small T. In $1d$ this agrees also with the exact low-temperature result[87]; see as well the discussion in[37] on the low temperature behaviour of $J_s(T)/J$. We also mention that Monte Carlo simulations[88] confirm that for low temperature one has that the slope $\partial J_s/\partial T$ for $T \to 0$ is 1/4, as given in (57).

In order to go beyond the saddle-point approximation, it is necessary to explicitly solve the flow Eq. (42). Then the expectation value κ_* for the field ρ is defined by the minimum

$$\left.\frac{\partial U_{k\to 0}(\rho)}{\partial \rho}\right|_{\kappa_*} = 0, \tag{58}$$

and the phase stiffness is given by (54).

Our results are summarized in Fig. 6 which shows the temperature dependence of the spin stiffness $J_s(T)$. In this figure the solid lines correspond to the results generated by amplitude fluctuations using Eq. (54), but without considering the vortex fluctuations. The different lines correspond to different approximations discussed in the following. The dashed lines represent the vortex renormalized stiffness and are obtained by considering

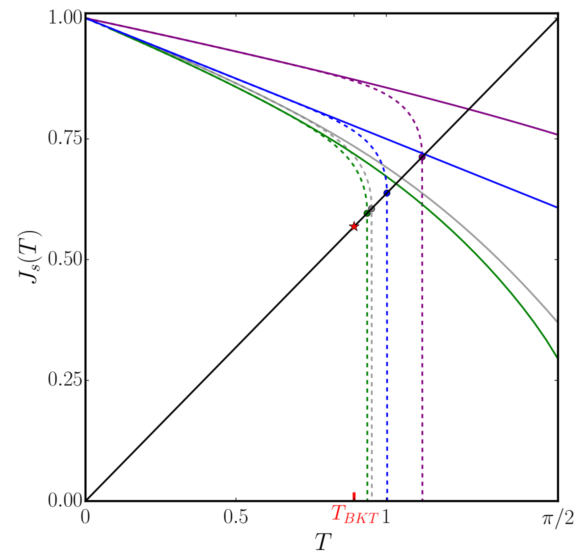

FIG. 6. Superfluid stiffness J_s in units of J as a function of the temperature for the XY model. The red lines represent the $|\varphi|^4$ model with initial condition (28) for the potential and $\mu = Jd$. The blue lines are the results from the low-temperature expansion (57). Finally, the green lines come again from the XY potential but quadratic dispersion relation with $\mu = 0$ chosen to match the low-temperature expansion as $T \to 0$. Solid and dashed lines represent respectively the results without and with the inclusion of vortex excitations.

the effect of vortex fluctuations via the perturbative SG Eqs. (35) and (36) with initial conditions (39) and (40) after performing the RG for the amplitude modes. Without vortex fluctuations the BKT temperature is simply obtained by the intersection of $J_s(T)$ with $\frac{2T}{\pi}$. From the top of the figure we have:

a. the results for the $|\varphi|^4$ model with initial potential (28) and $\mu = Jd$ (purple lines);

b. the low-temperature expansion (57) (blue lines);

c. an analytical approximation obtained determining the stiffness via a mean-field estimate of $J_s(T)$, as described below (gray lines);

d. the FRG results obtained for $\mu = 0$ (green lines).

In Fig. 6 we also plot for comparison the Monte Carlo result for $T_{\rm BKT}$.

A remark is in order here: when mapping the XY model onto the two-component $|\varphi|^4$ lattice field theory in section III, we underlined that the mapping is exact and the results should be μ independent as long as $\mu \geq Jd$. However, as discussed above, our FRG flow equation for the action (30) is applied to the XY model by modifying only the initial condition for the bare potential. This procedure is incomplete since the lattice field theory equivalent of the XY model has the lattice dispersion (26) rather than the continuous one (27). Therefore, the application of the FRG flow with continuous dispersion (27) and $\mu = Jd$ (red line in Fig. 6) is a rather crude approximation and does not agree with the low-temperature expansion (blue line).

Moreover, approximating the lattice dispersion with a continuous dispersion introduces a μ dependence in our result. We can exploit this and fix $\mu = 0$ to approach the exact low-temperature asymptotics. While such a value of μ would not be allowed in the lattice theory with dispersion (26), it is permitted in the continuous case. The resulting green solid line in Fig. 6 shows a consistent improvement over the low-temperature expansion (blue line).

Since the effect of the amplitude flucututations in the continuous $|\varphi|^4$ model with effective potential (28) is rather small, we expect that analytic results for the superfluid stiffness obtained from the saddle point solution follow very closely the exact results in all the range of the temperature between zero and $T_{\rm BKT}$. This can be made quantitative by observing that one could obtain very good results (plotted as gray lines in Fig. 6) by solving the following mean-field equation for the superfluid stiffness $J_s(T)/J$:

$$J_s(T) = J\,\frac{I_1\left(4\beta J_s(T)\right)}{I_0\left(4\beta J_s(T)\right)} \tag{59}$$

(which is the solid gray line), and then use it as initial condition in the perturbative SG Eqs. (35)–(36). The procedure gives the dashed gray line and $T_{\rm BKT} = 0.96 \pm 0.02$, worse than the value (60) we find using $\mu = 0$, but again reasonably good.

Our results for the critical temperature of the BKT transition in the different approximations are:

a. $T_{\rm BKT}/J = 1.19 \pm 0.02$ (dashed purple line);

b. $T_{\rm BKT}/J = 1.00 \pm 0.02$ (dashed blue line);

c. $T_{\rm BKT}/J = 0.96 \pm 0.02$ (dashed gray line);

d. $T_{\rm BKT}/J = 0.94 \pm 0.02$ (dashed green line).

In conclusion our most accurate results, coming from the nonperturbative evaluation of the RG flow for the amplitude mode plus the RG flow for the phase using the perturbative SG results is the following:

$$\frac{T_{\rm BKT(FRG)}}{J} = 0.94 \pm 0.02 \tag{60}$$

in good agreement with the expected result for the XY model $T_{\rm BKT} \simeq 0.893J$ obtained by MC simulations[69–73]. It is worth noting that this very good agreement for the critical temperature has been obtained by matching with the appropriate choice of μ the low-temperature behaviour of the superfluid stiffness.

VI. CONCLUSIONS

The topological phase transition in two-dimensional spin models with continuous symmetry as explained by the Berezinskii, Kosterlitz and Thouless (BKT) theory is a celebrated result. Our aim in this paper has been to set up and implement a renormalization group framework for the BKT universality class to quantitatively determine nonuniversal properties such as the temperature dependence of the superfluid fraction, the critical chemical potential and the transition temperature, given their relevance in $2d$ physical realizations of BKT physics and in current experiments.

After discussing the role of the parametrization of the field in functional RG approaches to $2d$ BKT phase transitions, we argue that the amplitude-phase (AP) Madelung representation of the field is the natural choice to study the contribution of longitudinal spin fluctuations to nonuniversal quantities and we show that amplitude fluctuations are gapped at the critical point. With the AP parametrization we have been able to study the RG flow directly in the relevant degrees of freedom: amplitude (density) fluctuations, longitudinal spin-waves, and vortex excitations, and discuss their mutual interplay.

As a preliminary step, we have derived an explicit mapping from the $2d$ lattice XY model to a continuum $|\varphi|^4$ field theory. While in three and higher dimensions this continuum limit is straightforward, in two dimensions the mapping depends, qualitatively and quantitatively, on nonuniversal ultraviolet details of the initial model. As a result, we have mapped the original XY coupling J to the initial superfluid stiffness ρ and interaction λ at scale Λ of the corresponding $|\varphi|^4$ model. Therefore, the RG equations are the same and only the initial conditions differ to characterize the XY and $|\varphi|^4$ models, so that they can be treated within the same formalism on equal footing.

We then proceeded to write the action in the amplitude and phase degrees of freedom and we have shown that amplitude excitations are gapped, such that the BKT behavior is correctly recovered as a transition and not as a crossover at large distances. This result is based on the explicit subtraction in the functional RG equations of the Gaussian energy. While this is mainly a technical point, we think it is an interesting one since (i) in many other applications such contributions do not have any physical effect in the determination of the critical properties of $O(N)$ models, and (ii) the AP representation provides a straightforward way to show this effect.

Our FRG procedure is then based on two steps: we first perform FRG on the amplitude part S_A of the action (32). We then insert the obtained stiffness into the phase part of the action, which is given by the spin-wave action (33) with the phase crucially considered as a periodic variable. This allows us to correctly take into account the compact nature of the phase variable and to use the results of the sine-Gordon model.

The combination of the nonperturbative functional RG study of the amplitude part of the action with perturbative flow for the sine-Gordon model is already sufficient to give rather good results for nonuniversal and universal quantities. In particular, we determined the critical chemical potential for the $|\varphi|^4$ model and the nontrivial universal parameters κ' and θ_0 defined in Eqs. (47) and (51). Our results for these two parameters are $\kappa'_{(\mathrm{FRG})} = 0.67 \pm 0.07$ and $\theta_{0(\mathrm{FRG})} = 1.033 \pm 0.032$, that should be compared with the Monte Carlo results $\kappa' = 0.61 \pm 0.01$ and $\theta_0 = 1.068 \pm 0.01$[60]. For the XY model we obtained the temperature dependence of the stiffness $J_s(T)$, which receives nonuniversal corrections from amplitude fluctuations. It reproduces the exact low-temperature limit and predicts the critical temperature with an error of $\approx 5\%$.

In conclusion, our findings confirm that amplitude fluctuations only result in a finite renormalization of the stiffness and do not completely deplete the superfluid fraction. We also find, without *a priori* assumptions, that amplitude fluctuations are frozen for the $|\varphi|^4$ model and yield effectively a phase-only model of spin-wave and vortex excitations. Finally, we showed that the combined use of the functional RG for the amplitude modes and of perturbative results for the sine-Gordon model allows one to quantify the effect of vortex excitations at finite temperature, which depends on the value of the vortex core energy and yields a further lowering of T_c[37]. Results for several universal and nonuniversal quantities are presented, with a very good agreement with known results.

To further improve the obtained results for both the $|\varphi|^4$ and the XY models one can insert nonperturbative effects in the sine-Gordon part of the RG flow. To this end, one should compute the anomalous dimension η in the nonperturbative RG flow of the sine-Gordon model. Moreover, for the XY model, one should include lattice effects which are beyond the scope of this paper. The study of lattice effects leads in a natural way to generalized sine-Gordon models, which we think is promising for future work. Although the obtained results are rather good, we think that the inclusion of nonperturbative treatment for the SG phase part of the action (and of the lattice effects for the XY model) may lead to further improvements, worthwhile to estimate.

In general, this work can provide a basis for future efforts to derive a generalized sine-Gordon model which comprehensively includes amplitude fluctuations on equal footing with phase fluctuations, and not as an initial condition from a previous RG step, as we did in this paper. In this way one should be be able to describe also the feedback of vortex excitations onto the amplitude fluctuations. We think that it would also be interesting to extend the results of this work to $2d$ quantum systems in order to quantitatively determine T_c as a function of interaction strength in ultracold Bose[7,8] and Fermi gases[9,89–93] and for out-of-equilibrium situations[94–96].

Acknowledgements. The authors wish to thank L. Benfatto, C. Castellani, N. Dupuis, G. Gori, Z. Gulacsi, H. Knörrer, J. Lorenzana, and I. Maccari for insightful discussions. We also thank M. Hasenbusch and N. Prokofev for useful correspondence. This work is part of and supported by the DFG Collaborative Research Centre "SFB 1225 (ISOQUANT)". T.E. thanks the Erwin-Schrödinger Institute in Vienna for hospitality in the initial stages of this work. This work was supported by the János Bolyai Research Scholarship of the Hungarian Academy of Sciences. A.T. and I.N. acknowledge support from Progetto Premiale ABNANOTECH. N.D. and A.T. thank the Institut Henri Poincaré - Centre Emile Borel for hospitality, where the final part of this work was done during the trimester "Stochastic Dynamics Out of Equilibrium".

Appendix A: Spin-wave approximation

The expression for the magnetization is given by

$$M_i = \left\langle \frac{e^{i\theta_i}}{2} \right\rangle + \left\langle \frac{e^{-i\theta_i}}{2} \right\rangle , \tag{A1}$$

while the expression of the spin-spin correlation function on the lattice is

$$G_{ij} = \langle \cos(\theta_i - \theta_j) \rangle . \tag{A2}$$

Both are conveniently rewritten in continuous notation as

$$F(x) = \int \mathcal{D}\theta \, e^{\int \left[-\frac{K}{2} (\nabla\theta)^2 + J(x')\theta(x') \right] d^d x'} \tag{A3}$$

with $J(x') = i\delta(x')$ and $J(x') = i\delta(x-x') - i\delta(x')$, where the two expressions are valid respectively for the magnetization and the two point correlation function. The integral in latter expression yields

$$F(x) = e^{\int \left[\frac{1}{2K} J(x')\mathcal{G}(x'-y')J(y') \right] d^d x' \, d^d y'} = \begin{cases} M(x) = e^{-\frac{1}{K}\mathcal{G}(0)} \\ G(x) = e^{\frac{1}{K}[\mathcal{G}(x) - \mathcal{G}(0)]} \end{cases} \tag{A4}$$

where

$$\mathcal{G}(x) = \int \frac{d^d q}{(2\pi)^d} \frac{e^{-i\boldsymbol{q}\cdot\boldsymbol{x}}}{q^2} \tag{A5}$$

(the $x = 0$ case must be evaluated separately in a finite volume and in the thermodynamic limit). In a finite system of size L we obtain in $d = 2$

$$G_L(0) = \frac{1}{2\pi} \log\left(\frac{L}{a} \right) \tag{A6}$$

leading to a vanishing magnetization in the $2d$ system in the thermodynamic limit.

In order to evaluate $\mathcal{G}(x)$ it is convenient to pursue the computation directly in the thermodynamic limit. We first consider a general dimension d and then compute the $d \to 2$ limit. One has then

$$\mathcal{G}(0) = \frac{s_d \pi^{d-2}}{d-2} a^{2-d}, \tag{A7}$$

where s_d is the surface of the d dimensional unit sphere divided by $(2\pi)^d$. The finite x expression can be obtained in the continuum limit $a \to 0$ as

$$\mathcal{G}(x) = \frac{s_d x^{2-d}}{(d-2)s_d}. \tag{A8}$$

One gets

$$\lim_{d\to 2} \left[\mathcal{G}(x) - \mathcal{G}(0)\right] = -\frac{1}{2\pi} \log\left(\frac{\pi x}{a}\right). \tag{A9}$$

Appendix B: Flow equations for the amplitude and phase scheme

In order to derive the FRG flow equations, we project the Wetterich Eq.[38] onto the theory space defined by the effective action ansatz (41) to obtain[39]

$$\partial_t U_k(\rho) = \frac{1}{2}\int \frac{d^d q}{(2\pi)^d}\left[\frac{\partial_t R_k^{(\theta)}(q)}{\rho\, q^2 + R_k^{(\theta)}(q)} + \frac{\partial_t R_k^{(\rho)}(q)}{(4\rho)^{-1}q^2 + U_k^{(2)}(\rho) + R_k^{(\rho)}(q)}\right]. \tag{B1}$$

We choose both regulators $R^{(\ell)}$ (with $\ell = \rho, \theta$) of the form

$$R_k^{(\ell)}(q) = \alpha_\ell (k^2 - q^2)\theta(k^2 - q^2), \tag{B2}$$

where α_ℓ is an appropriate dimensional constant necessary to have the correct dimension in the regulator terms. The regulator scale derivative is

$$\partial_t R_k^{(\ell)}(q) = -(2\,\alpha_\ell - \partial_t \alpha_\ell) k^2 \theta(k^2 - q^2). \tag{B3}$$

The flow for the effective potential in $d = 2$ reads (for $\partial_t \alpha_\ell = 0$)

$$\partial_t U_k(\rho) = -\frac{k^2}{4\pi}\left(\frac{\alpha_\theta \log\left(\frac{\rho}{\alpha_\theta}\right)}{\rho - \alpha_\theta} + \frac{4\alpha_\rho \rho \log\left(1 + \frac{4\alpha_\rho \rho - 1}{4\rho U_k''(\rho)/k^2 + 1}\right)}{4\alpha_\rho \rho - 1}\right). \tag{B4}$$

This equation is solved numerically for the full potential function to produce the results shown. Nevertheless, in order to gain a qualitative understanding of the flow, it is useful to employ a second-order Taylor expansion around the running potential minimum

$$U_k(\rho) = \frac{\lambda_k}{2}(\rho - \kappa_k)^2, \tag{B5}$$

which leads to the following flowing RG couplings:

$$\partial_t \kappa_k = -\frac{\partial_t U_k^{(1)}(\kappa_k)}{U_k^{(2)}(\kappa_k)}, \tag{B6}$$

$$\partial_t \lambda_k = \partial_t U_k^{(2)}(\kappa_k) + U_k^{(3)}(\kappa_k)\partial_t \kappa_k. \tag{B7}$$

The general flow equation (B4) contains two free parameters $\alpha_{\theta,\rho}$, which are dimensionless in $d = 2$. The phase diagram in Figs. 3 has been obtained with $\alpha_\theta = \kappa_k$ and $\alpha_\rho = 1/(4\kappa_k)$ in order to simplify the flow equations, but different choices of these parameters give equivalent results.

1. D. J. Bishop and J. D. Reppy, Phys. Rev. Lett. **40**, 1727 (1978).
2. K. Epstein, A. M. Goldman, and A. M. Kadin, Phys. Rev. Lett. **47**, 534 (1981).
3. D. J. Resnick, J. C. Garland, J. T. Boyd, S. Shoemaker, and R. S. Newrock, Phys. Rev. Lett. **47**, 1542 (1981).
4. P. Martinoli and C. Leemann, J. of Low Temp. Phys. **118**, 699 (2000).
5. R. Fazio and H. van der Zant, Phys. Rep. **355**, 235 (2001).
6. E. Simanek, *Inhomogeneous superconductors: granular and quantum effects* (Oxford University Press, Oxford, 1994).
7. Z. Hadzibabic, P. Krüger, M. Cheneau, B. Battelier, and J. Dalibard, Nature **441**, 1118 (2006).
8. V. Schweikhard, S. Tung, and E. A. Cornell, Phys. Rev. Lett. **99**, 030401 (2007).
9. P. A. Murthy, I. Boettcher, L. Bayha, M. Holzmann, D. Kedar, M. Neidig, M. G. Ries, A. N. Wenz, G. Zürn, and S. Jochim, Phys. Rev. Lett. **115**, 010401 (2015).
10. T. Giamarchi, *Quantum physics in one dimension* (Oxford University Press, Oxford, 2004).
11. D. R. Nelson, *Defects and geometry in condensed matter physics* (Cambridge University Press, Cambridge, 2002).
12. N. D. Mermin and H. Wagner, Phys. Rev. Lett. **17**, 1133 (1966).
13. P. C. Hohenberg, Phys. Rev. **158**, 383 (1967).
14. V. L. Berezinskii, Sov. Phys. JETP **34**, 610 (1972).
15. J. M. Kosterlitz and D. J. Thouless, J. Phys. C **6**, 1181 (1973).
16. J. M. Kosterlitz, J. Phys. C **7**, 1046 (1974).
17. J. M. Kosterlitz, Rep. Progr. Phys. **79**, 026001 (2016).
18. Royal Swedish Academy of Sciences (2016), URL `http://www.nobelprize.org/nobel_prizes/physics/laureates/2016/advanced.html`.
19. O. Penrose and L. Onsager, Phys. Rev. **104**, 576 (1956).
20. S. Stringari, in *Bose-Einstein condensation*, edited by A. Griffin, D. W. Snoke, and S. Stringari (Cambridge Uni-

versity Press, Cambridge, 1995).
[21] D. R. Nelson and J. M. Kosterlitz, Phys. Rev. Lett. **39**, 1201 (1977).
[22] S. T. Bramwell and P. C. W. Holdsworth, J. Phys.: Cond. Mat. **5**, L53 (1993).
[23] M. Tinkham, *Introduction to superconductivity* (McGraw-Hill, New York, 1996).
[24] W. E. Lawrence and S. Doniach, in *Proceedings of the 12th International Conference on Low Temperature Physics* (Tokyo, 1971), p. 361.
[25] L. Benfatto, C. Castellani, and T. Giamarchi, Phys. Rev. Lett. **98**, 117008 (2007).
[26] S. Coleman, Phys. Rev. D **11**, 2088 (1975).
[27] R. Rajaraman, *Solitons and instantons: an introduction to solitons and instantons in quantum field theory* (North-Holland, Amsterdam, 1987).
[28] J. Villain, J. Phys. **36**, 581 (1975).
[29] J. V. José, L. P. Kadanoff, S. Kirkpatrick, and D. R. Nelson, Phys. Rev. B **16**, 1217 (1977).
[30] P. Minnhagen, Rev. Mod. Phys. **59**, 1001 (1987).
[31] Z. Gulácsi and M. Gulácsi, Adv. Phys. **47**, 1 (1998).
[32] J. Fröhlich and T. Spencer, Commun. Math. Phys. **83**, 411 (1982).
[33] D. J. Amit, Y. Y. Goldschmidt, and S. Grinstein, J. Phys. A: Math. Gen. **13**, 585 (1980).
[34] I. Nándori, J. Polonyi, and K. Sailer, Phys. Rev. D **63**, 045022 (2001).
[35] M. Le Bellac, *Quantum and statistical field theory* (Clarendon, Oxford, 1991).
[36] T. Schneider and J. M. Singer, *Phase Transition Approach to High Temperature Superconductivity* (Imperial College Press, London, 2000).
[37] L. Benfatto, C. Castellani, and T. Giamarchi, in *40 Years of Berezinskii-Kosterlitz-Thouless Theory* (World Scientific, Singapore, 2012), pp. 161–199.
[38] C. Wetterich, Phys. Lett. B **301**, 90 (1993).
[39] J. Berges, N. Tetradis, and C. Wetterich, Phys. Rep. **363**, 223 (2002).
[40] P. Kopietz, L. Bartosch, and F. Schütz, *Introduction to the Functional Renormalization Group* (Springer, Heidelberg, 2010).
[41] W. Metzner, M. Salmhofer, C. Honerkamp, V. Meden, and K. Schönhammer, Rev. Mod. Phys. **84**, 299 (2012).
[42] I. Boettcher, J. M. Pawlowski, and S. Diehl, Nucl. Phys. B **228**, 63 (2012).
[43] B. Delamotte, in *Renormalization Group and Effective Field Theory Approaches to Many-Body Systems* (Springer, Berlin, 2012), pp. 49–132.
[44] T. R. Morris and M. D. Turner, Nucl. Phys. B **509**, 637 (1998).
[45] A. Codello and G. D'Odorico, Phys. Rev. Lett. **110**, 141601 (2013).
[46] A. Codello, N. Defenu, and G. D'Odorico, Phys. Rev. D **91**, 105003 (2015).
[47] N. Defenu, A. Trombettoni, and A. Codello, Phys. Rev. E **92**, 1 (2015).
[48] N. Defenu, A. Trombettoni, and S. Ruffo, Phys. Rev. B **94**, 224411 (2016).
[49] M. Gräter and C. Wetterich, Phys. Rev. Lett. **75**, 378 (1995).
[50] G. v. Gersdorff and C. Wetterich, Phys. Rev. B **64**, 054513 (2001).
[51] H. C. Krahl and C. Wetterich, Phys. Lett. A **367**, 263 (2007).
[52] S. Nagy, I. Nándori, J. Polonyi, and K. Sailer, Phys. Rev. Lett. **102**, 241603 (2009).
[53] T. Machado and N. Dupuis, Phys. Rev. E **82**, 041128 (2010).
[54] P. Jakubczyk, N. Dupuis, and B. Delamotte, Phys. Rev. E **90**, 062105 (2014).
[55] P. Jakubczyk and W. Metzner, Phys. Rev. B **95**, 085113 (2017).
[56] N. Defenu, P. Mati, I. G. Márián, I. Nándori, and A. Trombettoni, J. High Energy Phys. **2015**, 141 (2015).
[57] J. C. Le Guillou and J. Zinn-Justin, Phys. Rev. B **21**, 3976 (1980).
[58] E. Brezin and J. Zinn-Justin, Phys. Rev. Lett. **36**, 691 (1976).
[59] N. Prokof'ev, O. Ruebenacker, and B. Svistunov, Phys. Rev. Lett. **87**, 270402 (2001).
[60] N. Prokof'ev and B. Svistunov, Phys. Rev. A **66**, 043608 (2002).
[61] S. Pilati, S. Giorgini, and N. Prokof'ev, Phys. Rev. Lett. **100**, 140405 (2008).
[62] A. Rançon and N. Dupuis, Phys. Rev. A **85**, 063607 (2012).
[63] V. N. Popov, *Functional integrals in quantum field theory and statistical physics* (Reidel, Dordrecht, 1983).
[64] D. S. Fisher and P. C. Hohenberg, Phys. Rev. B **37**, 4936 (1988).
[65] G. Baym, J.-P. Blaizot, M. Holzmann, F. Laloë, and D. Vautherin, Phys. Rev. Lett. **83**, 1703 (1999).
[66] S. T. Bramwell and P. C. W. Holdsworth, Phys. Rev. B **49**, 8811 (1994).
[67] A. Trombettoni, A. Smerzi, and P. Sodano, New J. Phys. **7**, 57 (2005).
[68] A. Pelissetto and E. Vicari, Phys. Rep. **368**, 549 (2002).
[69] R. Gupta, J. DeLapp, G. G. Batrouni, G. C. Fox, C. F. Baillie, and J. Apostolakis, Phys. Rev. Lett. **61**, 1996 (1988).
[70] N. Schultka and E. Manousakis, Phys. Rev. B **49**, 12071 (1994).
[71] P. Olsson, Phys. Rev. B **52**, 4526 (1995).
[72] M. Hasenbusch, J. Phys. A: Math. Gen. **38**, 5869 (2005).
[73] Y. Komura and Y. Okabe, J. Phys. Soc. Japan **81**, 113001 (2012).
[74] H. Kleinert, *Gauge Fields in Condensed Matter* (World Scientific, Singapore, 1989).
[75] W. Janke and K. Nather, Phys. Rev. B **48**, 7419 (1993).
[76] J. Zinn-Justin, *Quantum Field Theory and Critical Phenomena* (Clarendon Press, Oxford, 1996).
[77] U. Jentschura, I. Nándori, and J. Zinn-Justin, Ann. Phys. **321**, 2647 (2006).
[78] S. Nagy, I. Nándori, J. Polonyi, and K. Sailer, Phys. Rev. D **77**, 025026 (2008).
[79] I. Nándori, S. Nagy, K. Sailer, and A. Trombettoni, Phys. Rev. D **80**, 025008 (2009).
[80] I. Nándori, S. Nagy, K. Sailer, and A. Trombettoni, J. High Energy Phys. **2010**, 69 (2010).
[81] V. Bacsó, N. Defenu, A. Trombettoni, and I. Nándori, Nucl. Phys. B **901**, 444 (2015).
[82] H. Nishimori and G. Ortiz, *Elements of phase transitions and critical phenomena* (Oxford University Press, Oxford, 2011).
[83] C. Mudry, *Lecture Notes on Field Theory in Condensed Matter Physics* (World Scientific, Singapore, 2014).
[84] N. V. Prokof'ev and B. V. Svistunov, Phys. Rev. B **61**, 11282 (2000).

[85] Z. Hadzibabic and J. Dalibard, Riv. del Nuovo Cim. **34**, 389 (2011).
[86] A. S. T. Pires, Phys. Rev. B **53**, 235 (1996).
[87] H. E. Stanley, Phys. Rev. **179**, 570 (1969).
[88] M. Hasenbusch, private communication (2017).
[89] M. Bauer, M. M. Parish, and T. Enss, Phys. Rev. Lett. **112**, 135302 (2014).
[90] M. G. Ries, A. N. Wenz, G. Zürn, L. Bayha, I. Boettcher, D. Kedar, P. A. Murthy, M. Neidig, T. Lompe, and S. Jochim, Phys. Rev. Lett. **114**, 230401 (2015).
[91] I. Boettcher, L. Bayha, D. Kedar, P. A. Murthy, M. Neidig, M. G. Ries, A. N. Wenz, G. Zuern, S. Jochim, and T. Enss, Phys. Rev. Lett. **116**, 045303 (2016).
[92] L. Madeira, S. Gandolfi, and K. E. Schmidt, arXiv:1703.01998 (2017).
[93] P. A. Murthy, M. Neidig, R. Klemt, L. Bayha, I. Boettcher, T. Enss, M. Holten, G. Zürn, P. M. Preiss, and S. Jochim (2017).
[94] H. C. Chu and G. A. Williams, Phys. Rev. Lett. **86**, 2585 (2001).
[95] L. He, L. M. Sieberer, and S. Diehl, Phys. Rev. Lett. **118**, 085301 (2017).
[96] T. Schweigler, V. Kasper, S. Erne, B. Rauer, T. Langen, T. Gasenzer, J. Berges, and J. Schmiedmayer, Nature (London) **545**, 323 (2017).